SEMARAK ILMU PUBLISHING

Journal of Advanced Research in Fluid Mechanics and Thermal Sciences

Journal homepage:
https://semarakilmu.com.my/journals/index.php/fluid_mechanics_thermal_sciences/index
ISSN: 2289-7879

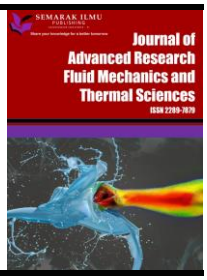

The Effect of Blended Palm Oil Biodiesel Droplet Properties on Evaporation Characteristics

Favian Jikol[1], Mohd Zaid Akop[1,*], Yusmady Mohamed Arifin[1], Mohd Azli Salim[1], Safarudin Gazali Herawan[2]

[1] Faculty of Mechanical Technology and Engineering, Universiti Teknikal Malaysia Melaka, 76100 Durian Tunggal, Melaka, Malaysia
[2] Industrial Engineering Department, Faculty of Engineering, Bina Nusantara University, Indonesia

ARTICLE INFO

Article history:
Received 27 September 2023
Received in revised form 30 November 2023
Accepted 17 December 2023
Available online 31 December 2023

Keywords:
Biodiesel; evaporation; heated surface; non-single droplet; single droplet

ABSTRACT

The evaporation characteristics of a single fuel droplet of diesel fuel (DF) and the Malaysian palm oil biodiesel-diesel blend (B10-B50) were studied experimentally. The fuel droplet properties consisted of different ratios of palm oil biodiesel mixtures which could influence the droplet behaviour when impinged on the heated surface. By employing the hot surface deposition test (HSDT) method, the droplets impinging on the heated surface of an aluminum alloy plate were observed to evaluate the droplet's evaporation characteristics including the evaporation lifetime and maximum evaporation point (MEP) of the tested fuels. Furthermore, the deposit's surface temperature for dry condition (t_{imp}=7 seconds) and wet condition (t_{imp}=3 seconds) test were also measured during the deposition test. Finally, the deposit development on the heated surface was evaluated through a logarithmic expression of $M_R/m_D = \alpha N_D^{\beta}$. The results showed that the evaporation lifetime of each test fuel decreased with increasing hot plate surface temperature. Furthermore, the MEP was the highest for B30 (380°C), followed by B20 and B40 (375°C), B10 and B50 (365°C), and DF (360°C). In the dry condition test, the recorded average minimum and maximum deposit surface temperatures were observed to be within the range of T_d=295°C to T_d=325°C for DF and T_d=290°C to T_d=350°C for B10-B50 fuels. On the other hand, for the wet condition test, the recorded average minimum deposit surface temperatures for both DF and B10-B50 fuels were consistently lower than the hot plate temperature. DF exhibited the most variation, ranging from T_d=200°C to T_d=300°C, whereas, for B10-B50, the recorded deposit surface temperature was only ranging from T_d=150°C to T_d=200°C.

1. Introduction

The unmanageable rate of fossil fuel use and the high levels of emissions produced by traditional energy sources directly contribute to global environmental damage [1]. Fossil fuel such as petroleum diesel is one of the main contributors to global air pollution. As diesel engine is widely operated especially in the transportation sector, a new kind of renewable energy should be implemented to

* *Corresponding author.*
E-mail address: zaid@utem.edu.my

https://doi.org/10.37934/arfmts.112.2.214229

minimize the dependence on fossil fuel. One of the sustainable energy sources with enormous potential to eventually replace liquid fossil fuels is palm oil biodiesel [2]. Malaysia is currently behind Indonesia as the largest crude palm oil producer and exporter in the world [3,4]. However, palm oil biodiesel might have different fuel properties compared to the common diesel found in the market, which can influence the performance of the engine operations. While the use of 100% biodiesel is not yet widespread in commercial vehicles, diesel-biodiesel blends ranging from 5% to 30% biodiesel mixed with pure diesel are globally accepted and employed with no or minor modification in diesel engines [5,6]. Moreover, the thermal efficiency of the engine, when fuelled by biodiesel blends, was comparable to that of pure diesel fuel [7]. As mentioned by Marlina *et al.,* [8], vegetable oils such as crude palm oil are dominated by saturated fatty acid contents. The fatty acid composition significantly influences the physical and chemical characteristics of vegetable oils such as the droplet's surface tension, evaporation, and atomization. Furthermore, the extended chain with numerous unsaturated double bonds in biodiesel contributes to elevated surface tension, impeding droplet formation and leading to sluggish evaporation rates, thereby compromising the efficiency of the atomization process. In another work on droplets suspended on a thermocouple, the same author also figured that adding an additive to the biodiesel could improve the evaporation characteristics [9]. The author found that adding 1.8-cineole in crude palm oil causes the rapid expansion and enlargement of trapped bubbles, hence accelerating the evaporation rate of the droplet. When applied in diesel engines, significant deposit formation could occur inside the combustion chamber eventually affecting the emissions and mechanical performance of the engine, as documented in our previous work [10].

Fuel properties have significant impacts on the evaporation characteristics of its droplet on a heated surface. The biodiesel-neat diesel blend fuel evaporation characteristics such as the evaporation lifetime are determined by the percentage of biodiesel in the blended mixture [11]. This implies that adding biodiesel to base diesel will increase fuel consumption due to the increased combustion rate. One of the most important reasons to study the evaporation characteristics or droplet-wall interaction of a single fuel droplet is to characterize the engine's spray vaporization and combustion as mentioned by Pan *et al.,* [12]. The author also mentioned that the dynamic of the droplet can be influenced by various factors such as the droplet's density and viscosity, diameter, velocity, and liquid film. On the other hand, the overall rate of fuel evaporation is also influenced by temperature, pressure, volatility, diameter of the spray drops, and the velocity of the drops in relation to the surrounding gas [13]. This is in agreement with Mariani *et al.,* [14] who mentioned that fuel properties such as the fuel droplet size and momentum are crucial in enhancing optimum fuel mixing and simultaneously reducing the droplet's interaction with the combustion chamber wall. Furthermore, a study on single-droplet combustion is crucial because single-droplet combustion shares many physical and chemical processes with spray characteristics [15]. However, this statement is opposite to that of Wang *et al.,* [16], who mentioned that, because the droplets around them have an impact on their evaporation and burning, spray combustion droplets are not the same as single, isolated droplets. Another study was conducted by Zhang *et al.,* [17] on a similar matter as investigation on droplet combustion is vital as it was the foundation of spray combustion for the real engine. Moreover, Wang *et al.,* [18] and He and Piao [19] also pointed out that the topic of droplet evaporation characteristics studies is the basis for understanding the complex combustion of liquid fuels and elaborating the behavior of internal combustion engine fuel injection systems and spray cooling.

Several factors could affect the evaporation characteristics of a particular fuel droplet, especially the droplet-surface behavior. During the evaporation of a single droplet fuel, there are two types of temperature regimes involved, which are the Nukiyama temperature and Leidenfrost temperature

as explained by Segawa *et al.,* [20]. Orzechowski [21] in his study also describes the Leidenfrost temperature regime during the evaporation process. Moreover, Mohaddes *et al.,* [22], mentioned the Leidenfrost effect, which causes the impinging spray to splash and rebound, or the creation of an evaporating fuel coating on the heated surface. Mach *et al.,* [23] also proposed that the droplet-surface behavior is characterized by Nukiyama temperature, which is the droplet boiling temperature at which the droplet has a minimum evaporation lifetime, and Leidenfrost temperature, where the droplet possesses a maximum evaporation lifetime and levitates above the surface on a layer of vapor, as illustrated in Figure 1. In the figure, it can be seen that the falling droplet is floating above a vapor layer, and most likely does not recoil anymore as the temperature of the heated surface is also decreased in this Leidenfrost temperature regime.

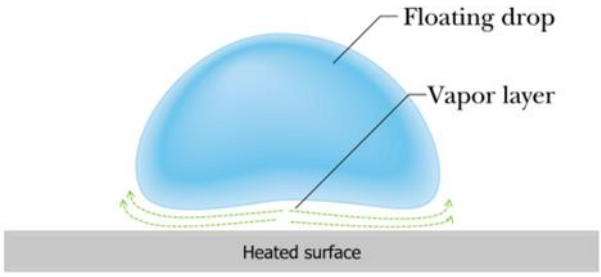

Fig. 1. Illustration of a droplet in Leidenfrost regime [24]

According to Bertola [25], the rebound phenomena at very high surface temperatures happen as a result of the impact-induced creation of a vapor film at the droplet-wall interface. This vapor layer functions as a sort of lubricant, minimizing energy loss during the spreading and gathering of the droplets. Another researcher, Mach *et al.,* [23] described that when a fuel droplet impinges on a metal surface, it may moisten the surface and spread, or it may wet the surface, cavitate, and then violently fragment, rebound intact, or splatter due to fragmentation at impact. The author also mentioned the importance of droplet-surface interactions in combustion chamber wall wetting and the point that it is more likely to occur on the part of walls with relatively lower temperatures. Additionally, he pointed out that in a high swirl engine, whether a droplet wets the surface or avoids contact with the wall and evaporates within the chamber depends on its kinetic energy, the temperature of the chamber wall, and the properties of the surface (previously produced deposits or oil layers). Furthermore, Chausalkar *et al.,* [26] mentioned that because individual droplets may wet the wall, bounce, or break up upon impact, the result of the spray impingement on walls over a variety of temperatures and ambient pressures can significantly influence the final air-fuel mixture quality. The total amount of pollutants released from the combustor can also be significantly influenced by the final rebound or deposition of these droplets on the combustor wall. For fuel injection systems, a lower droplet adherence to the surface is preferred because it allows for a more effective evaporation process.

In the work carried out by Reis [24], the author listed out the main forces in the droplet impact on a heated surface, as presented in Figure 2, which the forces are inertia, surface tension, viscosity, and adhesion, respectively. He also stated that numerous factors, including droplet diameter, impact velocity, saturation temperature, viscosity, and surface tension, which are directly related to the liquid characteristics, determine these forces in this process. Regarding the forces in droplets, Liang and Mudawar [27] described that the impact droplet dynamic is also heavily influenced by solid surface properties such as diffusivity, wettability, surface roughness, and surface temperature. These statements show that the evaporation characteristics of a fuel droplet on a heated surface do not

depend solely on its properties but are also influenced by the condition of the heated surface to which the droplet will be impinged.

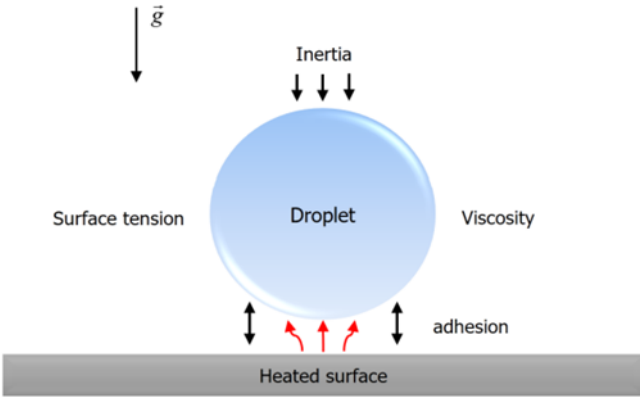

Fig. 2. Main forces in the droplet impact on a heated surface [24]

The studies on evaporation characteristics of palm oil biodiesel blend droplets on a heated surface were still limited, especially up to 20% blend ratio. Thus, this study aims to investigate the droplet evaporation characteristics of the Malaysian palm oil biodiesel-diesel blend on a heated aluminum alloy surface by using the Hot Surface Deposition Method (HSDT) in particular. Furthermore, the effect of impingement interval on the deposit development and the deposit's surface temperature will be examined. The results will be compared to those of neat diesel fuel to identify the influence of palm oil biodiesel blend droplet properties on droplet evaporation behavior at certain temperatures. Furthermore, the outcomes of this study are important as a reference in the real fuel deposition test.

2. Methodology

All fuels used in this experiment were obtained from the local factory in Malaysia. The diesel fuel (DF) used was pure diesel which was obtained directly from the refinement factory. On the other hand, the blended palm oil biodiesel fuels were produced by mixing neat diesel with processed Malaysian crude palm oil at room temperature. The biodiesel-diesel blend was a mixture of 10% of palm oil biodiesel with 90% of neat diesel by volume for the B10 fuel. The other fuel blends were prepared by blending the palm oil biodiesel with volume proportions of 20%, 30%, 40%, and 50% in neat diesel fuel, and designated as B20, B30, B40, and B50, respectively. The physicochemical properties of Malaysian palm oil biodiesel fuels are presented in Table 1.

Table 1
Physicochemical properties of DF and blended Malaysian palm oil biodiesel [28]

Properties	Fuel					
	DF	B10	B20	B30	B40	B50
Density (kg/m^3)	847	850	853	857	860	863
Kinematic viscosity (mm^2/s)	3.8	3.86	3.91	3.95	4	4.61
Heating value (MJ/kg)	45.21	44.23	44.12	43.13	42.95	42.74
Acid value (mg KOH/g)	0.16	0.18	0.22	0.26	0.3	0.33

On the other hand, the mass of 100 fuel droplets is measured using a microbalance scale, and three readings are taken for each test fuel to calculate the average mass. Due to the irregularities in droplet shapes and the challenges associated with measuring the actual diameter of each droplet without the assistance of a high-speed image processor, the sphericity value is considered negligible. In this research, the droplet is assumed to be a sphere for simplification. Before conducting the evaporation test, the mass and diameter of an individual fuel droplet are determined based on the fuel density and the mass of 100 droplets, as outlined in Eq. (1). The droplet properties are shown in Table 2 and it can be seen that a higher blending ratio of the biodiesel-diesel blend does not guarantee a heavier mass or larger droplet diameter, respectively.

$$m_D = (1/6\pi)(D_d)^3(\rho_{fuel}) \quad (1)$$

m_D = mass of a single fuel droplet (g)
D_d = diameter of single droplet (mm)
ρ_{fuel} = density of fuel (kg/m^3)

Table 2
Single fuel droplet properties

Fuel	Mass of single droplet, m_d (mg)	Diameter of a single droplet, D_d (mm)
DF	4.9	2.2
B10	5.3	2.3
B20	4.7	2.2
B30	4.8	2.2
B40	5.0	2.2
B50	4.9	2.2

The experimental method implemented in this study was the HSDT method. In the literature, the HSDT experimental concept has been applied in previous works regarding the investigation of fuel deposition on a heated wall surface [29-32]. As can be seen in the schematic diagram in Figure 3, the main experimental concept of this method was to investigate the fuel droplet mechanism when it was impinged on the heated aluminum alloy hot plate, which represents the pistons inside of the internal combustion (IC) engine. Aluminum alloy was used to fabricate the hot plate, pistons are mostly made of aluminum alloy [33,34]. The hot plate was electrically heated by a set heater of block which is located beneath the plate while the temperature was set and controlled on the control panel of the HSDT machine. The droplet was released from the needle tip and the evaporation process occurred on the center part of the hot plate was observed, which is the hottest region when heated as we identified in our previous studies [35,36]. The fixed distance between the hot plate's surface and the needle tip was L_h=80mm. Such distance aimed to address specific concerns. When the distance is below L_h=80mm, there is a higher chance of a wet condition as fuel droplets reach the plate's surface more quickly, regardless of the prolonged impingement interval. Conversely, distances exceeding L_h=80mm may result in more splash loss of impinged droplets, potentially affecting the precise measurement of the actual deposit production.

For this test, the initial test temperature was set at T_s=250°C, and a fuel droplet was impinged on the hot plate. The droplet evaporation behavior was observed and recorded. The droplet evaporation lifetime was manually measured using a digital stopwatch. To ensure data reliability, a minimum of three readings for droplet lifetime were taken at each test temperature. In the case of diesel fuel, the duration from when the droplet first makes contact with the hot plate surface until the completion of the evaporation process is considered the droplet's lifetime. However, for multi-

component fuels like palm oil biodiesel-diesel fuel blends, the droplet lifetime is recorded until the residual fuel becomes hard to vaporize, and no further vapor is produced during the evaporation process. With an increment of 5°C, the experiment was conducted until T_s=430°C of hot plate temperature. Other than that, the surface roughness of the hot plate surface and velocity of the impinging droplet were the constant variables in this test as those parameters could affect the evaporation characteristics of droplets as studied by Fukuda *et al.,* [37]. By analyzing the single fuel droplet behavior on the heated plate, the average evaporation lifetime, t_{life}, maximum evaporation point (MEP), and evaporation state can be obtained for each fuel.

To investigate the deposit formation, a multi-droplet of fuel must be impinged on the hot plate at different parameters which are the hot plate temperature, droplet interval, and fuel properties. Therefore, for each test fuel, the experiment was conducted until droplet N_D=16000 for both the dry condition (impingement interval t_{imp}=7 seconds) and wet condition (impingement interval t_{imp}=3 seconds) test. Moreover, the set temperature of the hot plate for B10-B50 fuel deposition tests is T_s=340°C, while for DF deposition tests is T_s=315°C.

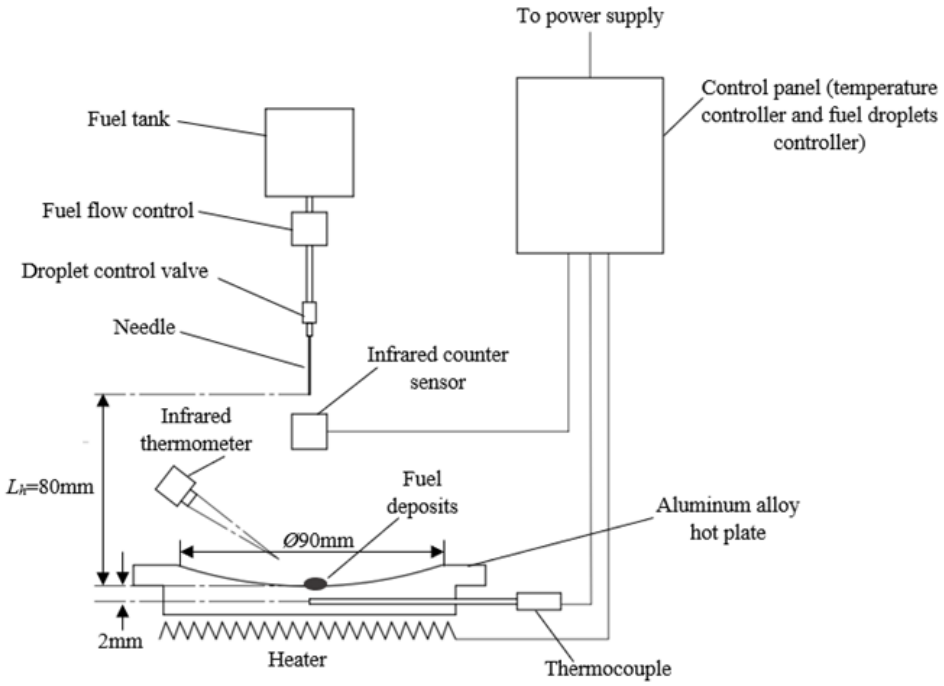

Fig. 3. Schematic diagram of experimental setup for HSDT

3. Results and Discussion

For all tested fuels, the droplet evaporation characteristics are presented in Figure 4(a) to Figure 4(f). These results are important as they will be used as a reference and to support the results in the actual fuel deposition test, whereas the initial wetting condition and the droplet's physical contact with the hot surface may be explained by these droplet properties. There are three main droplet characteristics shown in the figure, which are the droplet average evaporation lifetime, MEP, and evaporation states. The evaporation states consist of single droplet (indicated by a black dot) and non-single droplet (indicated by a white dot) as presented in the results in Figure 4(a) to Figure 4(f). The single droplet evaporation indicates a state of single droplet evaporation, where the surface temperature falls below the MEP temperature causing the fuel droplet to become stuck on the heated surface, as depicted in the illustration made by Arifin and Arai [38] in Figure 5(A1) (lens-shaped droplet and vapor bubble formation) and Figure 5(A2) (vigorous boiling droplet). Khavari *et*

al., [39] also mentioned that the formation of microscopic vapor bubbles at the solid-liquid interface during droplet spread at the surface is implied by the boiling phenomena that occur when a droplet impacts a heated surface, which occurs at high surface temperatures. After reaching the MEP temperature, fuel vapor is formed as illustrated in Figure 5(A3). Single droplet evaporation in this state indicated that the fuel droplet vaporizes with a spherical shape droplet and detaches from the heated surface. On the other hand, for non-single droplets, this symbol represents the ferocious boiling within the nucleate boiling regime (near MEP region) that results in a splashing of tiny droplets or broken film or fuel as can be seen in illustrations Figure 5(B1) and Figure 5(B2), respectively [40]. However, after the MEP region, the non-single droplet symbol illustrated in Figure 5(B3) means a break-up behavior of the fuel droplet [41,42].

The experiment started with a low surface temperature of the aluminum alloy. Fuel droplet remains on the heated surface for a longer duration at lower temperatures due to a prolonged evaporation lifespan. This might change the way that subsequent droplets evaporate as well as the way that deposits accumulate. As presented in Figure 4(a), when the hot plate surface temperature was increased, the DF evaporation lifetime gradually decreased. At the initial hot surface temperature of T_s=250°C, the average evaporation lifetime of DF was around t_{life}=40s, which was the lowest compared to the other test fuels. Before the experiment started, we expected that the droplet evaporation lifetime would be higher for fuel with higher biodiesel content. However, the results obtained indicated that the average evaporation lifetime at T_s=250°C of B30 fuel was the longest which was approximately t_{life}=75s, followed by the other fuels with an average evaporation lifetime of t_{life}=69s (B40), t_{life}=67s (B20 and B50), and t_{life}=61s (B10). Furthermore, the droplet evaporation lifetime profile for all tested fuels showed a gradual decrease, except for B40 fuel (Figure 4(e)) which indicated a steep curve between the surface temperature of T_s=280°C-300°C. This means that B40 lifetime decreases faster compared to other fuels in that temperature region.

The MEP, which is the maximum evaporation rate point (MEP) temperature is defined as the temperature at which a fuel droplet impinged on it evaporated with the shortest lifespan as illustrated in Figure 5. In addition, this point also demonstrated the upper bound on the ability of fuel droplets to adhere to a heated surface during evaporation. Due to the creation of fuel vapor between the fuel droplet and the hot wall surface after reaching this temperature, the fuel droplet began to separate from the wall surface. The obtained MEP for the tested fuels were 360°C (DF), 365°C (B10 and B50), 375°C (B20 and B40), and 385°C (B30). Surprisingly, despite not having the highest blending ratio, B30 fuel indicated MEP was the highest compared to B40 and B50, respectively. Moreover, the MEP of B50 was only around 5°C higher compared to DF. This shows that fuel properties in terms of blending ratio did not have a significant impact on the droplet MEP. However, it cannot be ruled out that other factors such as auto-oxidation might have altered the fuel physicochemical properties of the fuel during storage, consequently affecting the droplet evaporation characteristics [43]. After the MEP region, there were slight increases in the average evaporation lifetime of all fuels, even though the hot surface temperature was increased. This is identical to the illustration in Figure 5, which indicates that the droplet's lifetime increased and reached the Leidenfrost point temperature after the MEP region. At some point, when the temperature is raised, the evaporation rate is reduced and the droplet lifetime is slightly extended [44].

In terms of the evaporation mechanism, DF droplet evaporation produced the most droplet splashes (indicated by the non-single droplet symbol) after the MEP region as shown in Figure 4(a). During this phase, the break-up of droplet occurs as shown in Figure 5(B3). In addition to the droplet break-up behavior, Kompinsky *et al.,* [45] in his studies explained that the droplet bounces off the surface during the splitting process as a result of the tremendous thermal energy being transmitted to it and the high pressure that is being built up underneath it. Moreover, DF also produced more

smoke during the evaporation process compared to B10-B50. Unlike DF, a non-single droplet evaporation pattern occurred before the MEP region for B10 fuel (Figure 4(b)). The non-single droplet evaporation pattern consists of deposit splashes as illustrated in Figure 5(B1). One of the possible reasons may be explained by the mass of the droplet of B10 which is the heaviest, resulting in higher impact when hitting the heated surface and consequently producing more droplet splashes. Furthermore, droplet splashes phenomena also contributed by the different chemical bonds of the biodiesel fuel, which leads to elevated surface tension, impeding droplet formation, and leading to sluggish evaporation rates as being reviewed by Wang *et al.,* [46]. The author also mentioned that uneven distribution of various components within the droplet's dynamics results in a gradient in surface tension, influencing the droplet's behavior when impacted on a heated surface. For B20 and B30 fuels in Figure 4(c) and Figure 4(d), an obvious non-single droplet pattern for B20 appeared before the MEP region, while the latter was observed after the MEP region even though the droplet properties of these fuels were almost identical in terms of droplet diameter and droplet mass. On the other hand, B50 fuel (Figure 4(f)) produced the lowest non-single droplet evaporation profile compared to other fuels.

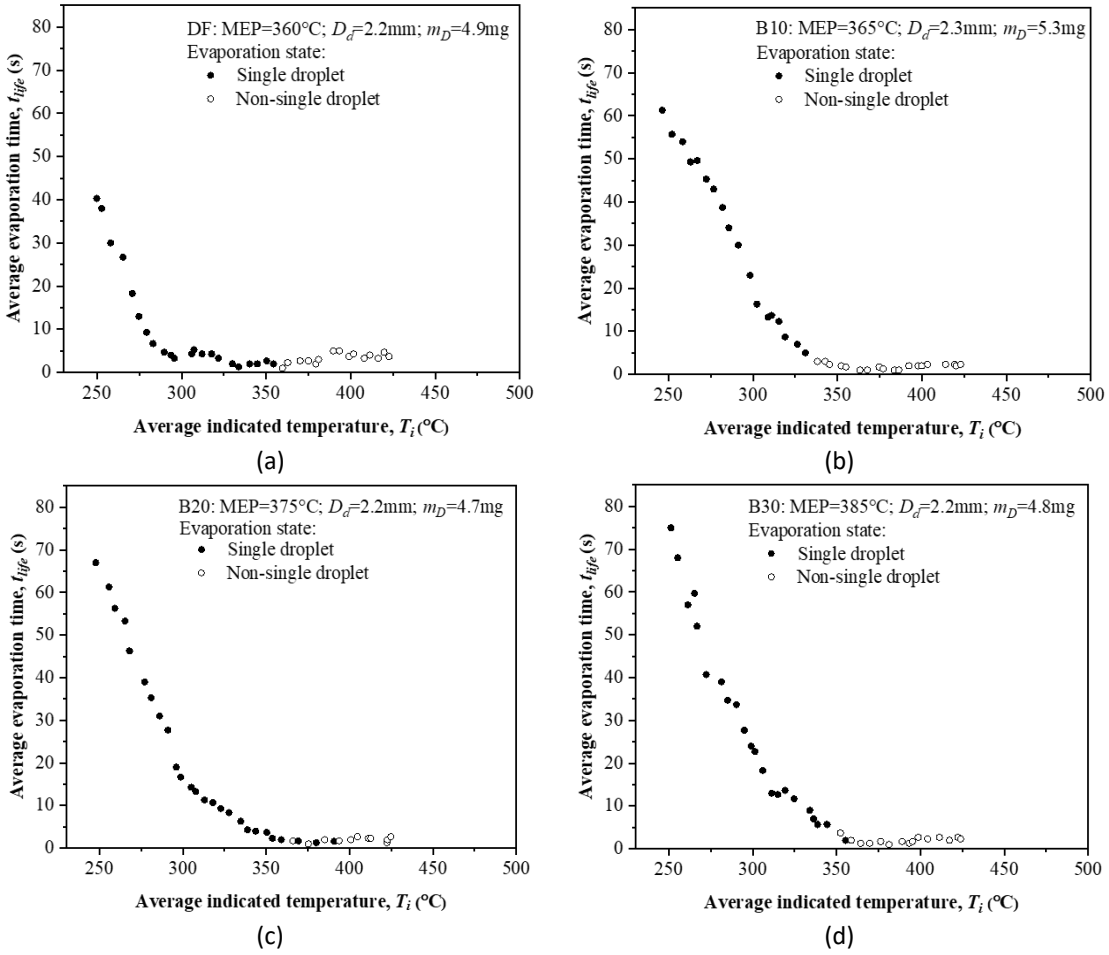

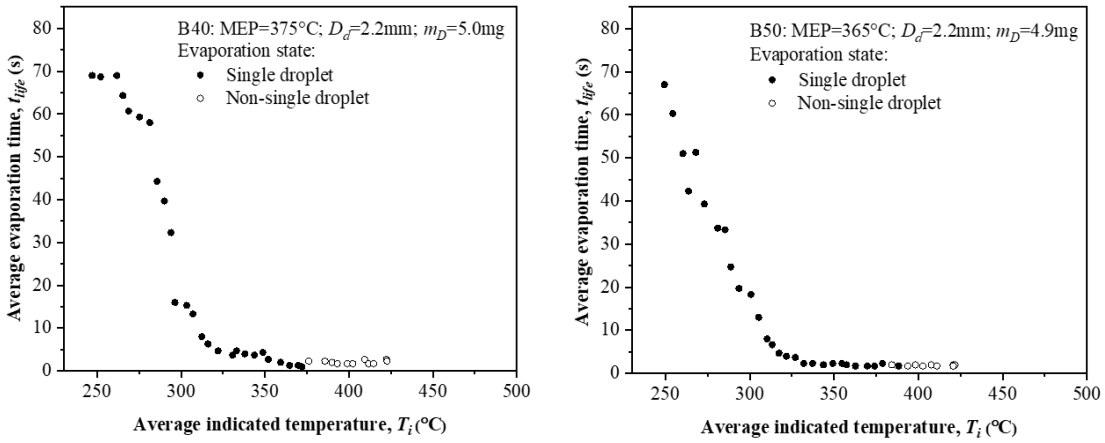

(e) (f)

Fig. 4. Evaporation characteristic of (a) DF, (b) B10, (c) B20, (d) B30, (e) B40, and (f) B50

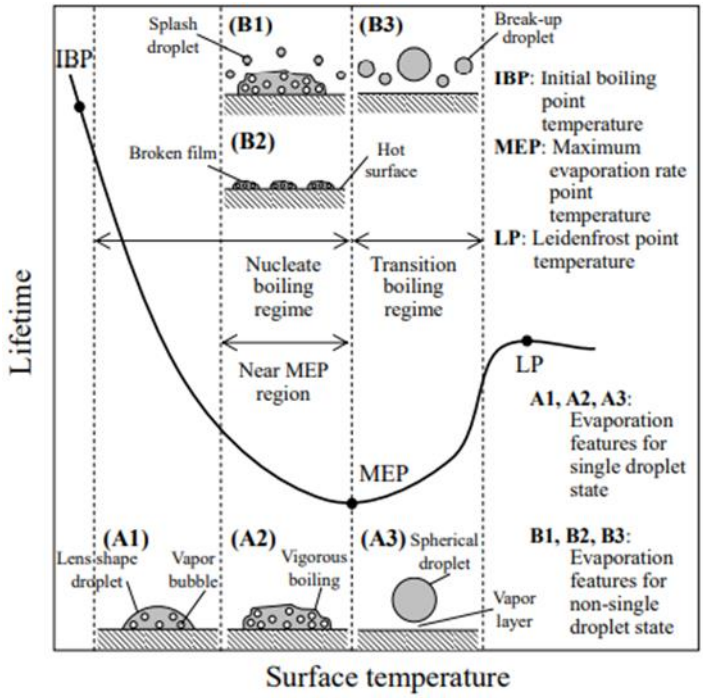

Fig. 5. General features for the single and non-single droplet states during fuel evaporation [38]

After the MEP values were obtained from the evaporation characteristics, parameters for the deposition experiment were determined. For DF, the hot plate surface temperature was T_s=315°C and for B10-B50, the temperature was T_s=340°C. The droplet impingement intervals for dry and wet conditions were similar for all test fuels. After the deposition test reached droplet N_D=1000, the mass and surface temperature of the generated deposit were recorded. This process was repeated for the next 1000 droplets until droplet N_D=16000. The recorded minimum and maximum deposit temperatures for each type of fuel are displayed in Figure 6 for the wet condition (t_{imp}=3 seconds) and Figure 7 for the dry condition (t_{imp}=7 seconds). These figures illustrate a consistent decreasing trend in recorded temperatures as the number of fuel droplets increases. In Figure 6(a), it is evident that the recorded average minimum deposit surface temperatures for both DF and B10-B50 fuels were consistently lower than the hot plate temperature, which was T_s=315°C for DF and T_s=340°C for the latter. Similarly, in Figure 6(b), the recorded average maximum temperatures of the deposits

formed on the hot plate surface were also lower than the set temperature of the hot plate. Among all the fuels tested in the wet condition, the average minimum and maximum deposit surface temperatures for DF exhibited the most variation, ranging from T_d=200°C to T_d=300°C. This variability may be attributed to the notably thin layer of DF deposits compared to the other fuels. For B10-B50 fuels, both the average minimum and maximum deposit surface temperatures were recorded below T_d=200°C, even though the set temperature of the hot plate for B10-B50 fuel deposition tests (T_s=340°C) was higher than that for DF deposition tests (T_s=315°C). In general, wet condition deposition tests resulted in the production of more deposits. Additionally, as the deposits became thicker and wet conditions persisted, the evaporation lifetime of fuel droplets increased, leading to a significant difference between the hot plate surface temperature and the deposit surface temperature. Moreover, the heat transfer behavior of the deposits also changed as the accumulated deposit amounts increased, leaving more liquid fuels on the hot plate surface [38,43].

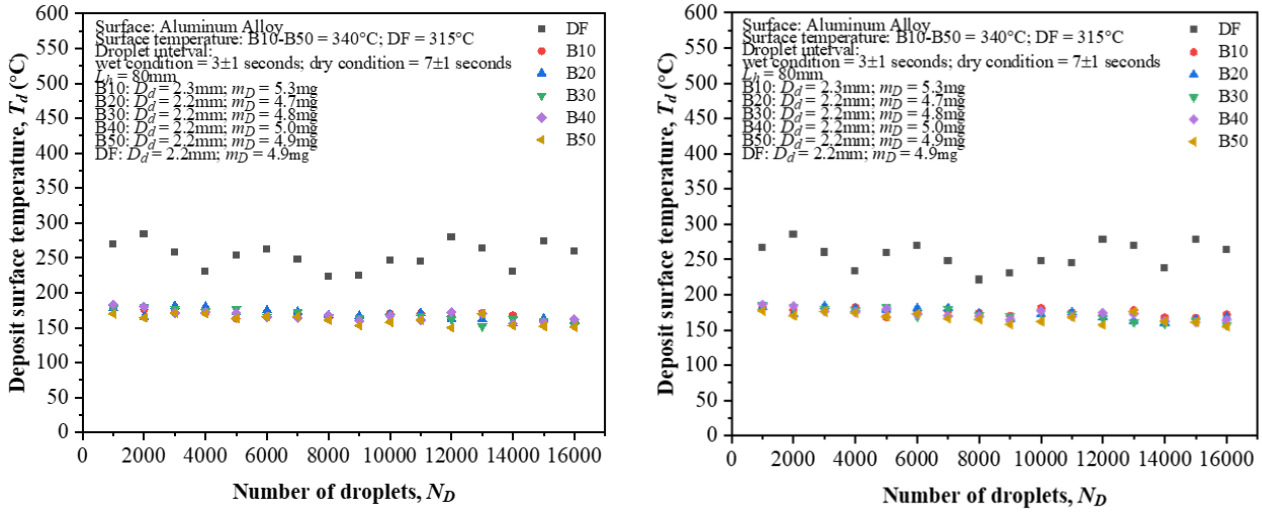

Fig. 6. (a) Minimum and (b) Maximum deposit surface temperature comparison for wet condition

In the dry condition test, the recorded average minimum and maximum deposit surface temperatures were observed to be within the range of T_d=295°C to T_d=325°C for DF and T_d=290°C to T_d=350°C for B10-B50 fuels, as depicted in Figure 7(a) and Figure 7(b). Notably, in this test, the average minimum and maximum deposit surface temperatures for DF displayed a higher degree of consistency. In comparison to the wet condition deposition test, the deposits formed by the tested fuels in the dry condition were notably fewer. Furthermore, these deposits appeared thinner in terms of physical characteristics and contained fewer liquid fuel remnants, especially when measuring the maximum deposit surface temperature, where there was hardly any observable accumulation of liquid fuel on the deposit surface. These conditions led to a reduced thermal impact on the oxidation of liquid fuels, despite the continuous oxidation of carbonaceous deposits. Additionally, as more deposits accumulated, the surface temperature experienced a slight decrease attributed to the impact of the deposits' low thermal conductivity [38,43].

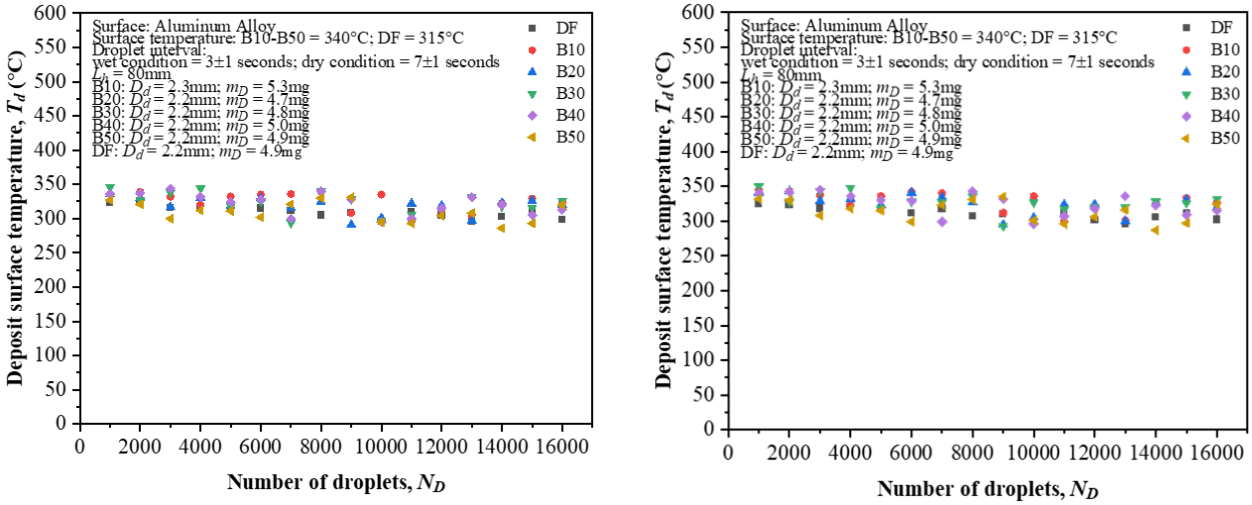

Fig. 7. (a) Minimum and b) Maximum deposit surface temperature comparison for dry condition

Eq. (2) was utilized to determine the value of α and β, with the value of m_D remaining constant throughout the test. It is solely dependent on the characteristics of the tested fuels for various HSDT settings [43]. Eq. (2) has also been applied in other works to depict deposit development on a hot surface [30,38,47,48]. These values are only suitable for droplet repetition for N_D=1000 and above due to the sensitivity of the microbalance. The parameter α signifies deposit formation during the early stages of the deposition, while the coefficient β is associated with the rate of deposit development. At the initial or early stage of the deposition test, there is no guarantee that fuel with a higher blend ratio will generate more deposits. Furthermore, at the later stage of the deposition test (droplet repetition N_D>16000), the thickness of the accumulated deposits will increase due to the extended droplet evaporation lifetime caused by the overlapping condition prior to increasing droplet number. In addition to that matter, the deposit development rate which corresponds to the value of β increases with significant value. Therefore, to minimize the rate of deposit formation, it is crucial to maintain a low value of β, especially at the later stage of deposition.

$$M_R/m_D = \alpha N_D^{\beta} \quad (2)$$

M_R = total deposits on a hot surface (g)
m_D = mass of a single fuel droplet (g)
N_D = number of impinged droplets
α = constant for initial deposition (-)
β = exponential index for deposition development (-)

The logarithmic expressions derived from the fuel deposition test, as shown in Figure 8 and Figure 9, are summarized in Table 3. Analyzing the values of the logarithmic expressions from Figure 8 and Figure 9, it is apparent that the slopes are directly related to the corresponding relative deposition mass (M_R) for each fuel. This indicates that as the number of fuel droplets increases, the mass of accumulated deposits also increases, but at varying rates of development. Additionally, the gap between the slopes provides insight into the rate of deposit development. For the wet condition test in Figure 8, there was a relatively narrow gap between the slopes for DF and B10 fuel, indicating that deposits developed at a comparable rate for these fuels. Similarly, B40 and B50 fuels also produced deposits with almost an equivalent rate of development. For B20 and B30 fuels, the deposit

development rate can be described as faster than that of DF and B10 fuels but slower compared to B40 and B50 fuels. In the dry condition test shown in Figure 9, there was no visible gap between the slopes for DF and B10 fuel. Similarly, B30 and B40 fuels also exhibited very narrow gaps between their slopes. However, for B20 and B50 fuels, wider gaps were observed compared to the other fuels. These observations provide insights into the relative rates of deposit development for different fuels under dry conditions.

In Table 3, for the dry condition (t_{imp}=7 seconds), deposition was notably influenced by the β value, as the β value increased for fuels with higher blend ratios. In terms of the α value, it decreased as the blend ratio increased, suggesting that it had a less significant impact on deposition. However, for the wet condition (t_{imp}=3 seconds), the expected trend of the β value increasing with the blend ratio was inconsistent. This inconsistency might be attributed to the early stages of the experiment (N_D < 5000), where fuels with lower blend ratios were able to produce more deposits. Furthermore, this indicates that a higher number of droplets may provide a better explanation for the correlation between α and β values. With more repetitions, different deposition trends can develop, especially in wet condition tests. Hence, it can be concluded that deposition is not solely dependent on the values of α and β, especially in tests with low droplet repetitions. Other factors, such as early stages of deposition also play a significant role in influencing the deposition process.

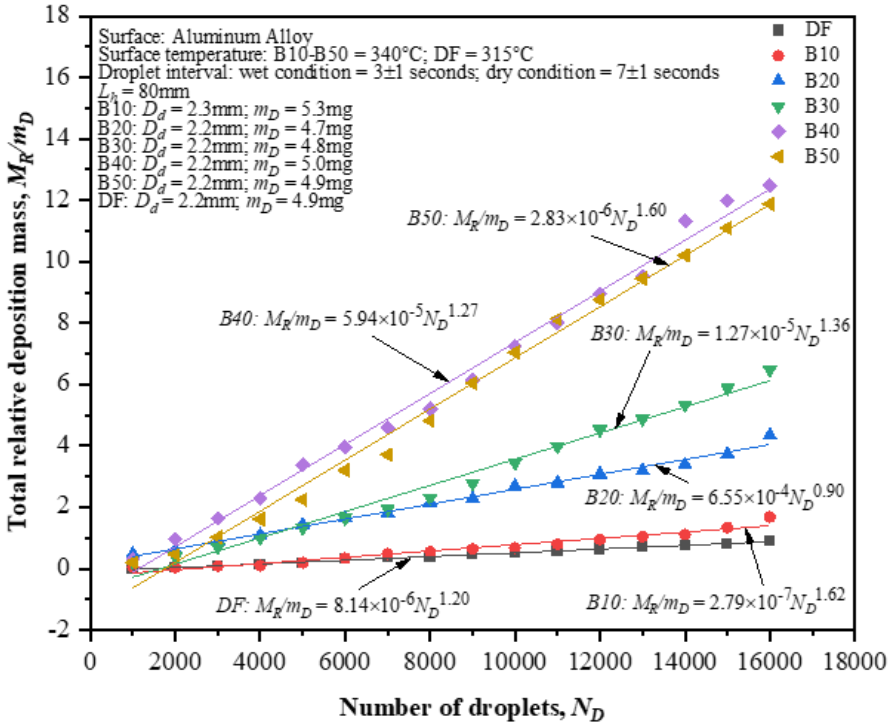

Fig. 8. Deposit development comparison for wet condition

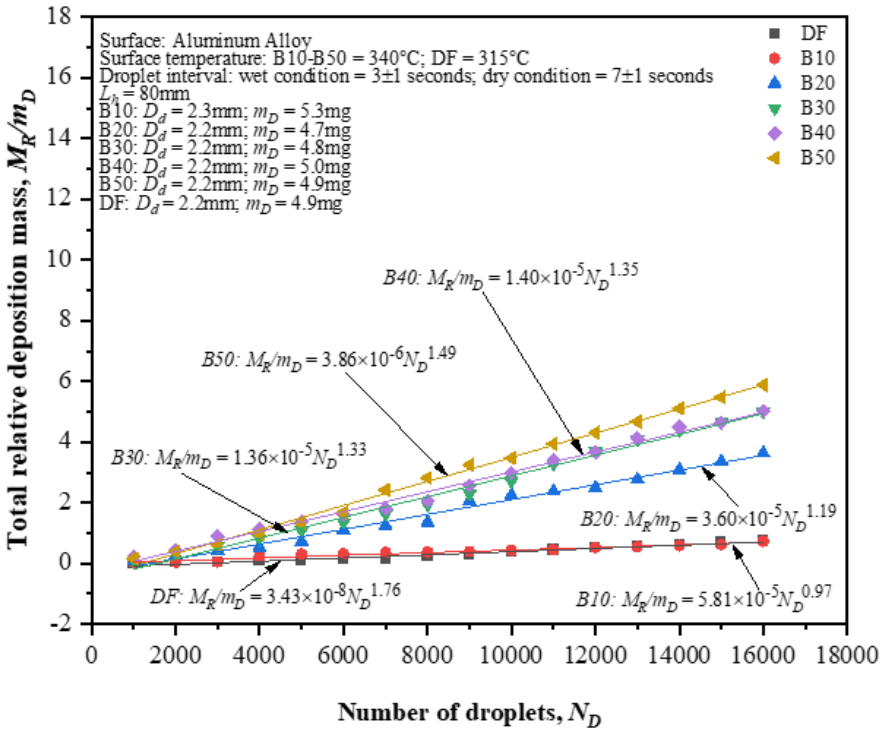

Fig. 9. Deposit development comparison for dry conditions

Table 3
Logarithmic expression values for N_D = 1000-16000

Fuel	Condition	α	β
DF	τ_{imp} = 3s, T_S = 315°C	8.14×10^{-6}	1.20
	τ_{imp} = 7s, T_S = 315°C	3.43×10^{-8}	1.76
B10	τ_{imp} = 3s, T_S = 340°C	2.79×10^{-7}	1.62
	τ_{imp} = 7s, T_S = 340°C	5.81×10^{-5}	0.97
B20	τ_{imp} = 3s, T_S = 340°C	6.55×10^{-4}	0.90
	τ_{imp} = 7s, T_S = 340°C	3.60×10^{-5}	1.19
B30	τ_{imp} = 3s, T_S = 340°C	1.27×10^{-5}	1.36
	τ_{imp} = 7s, T_S = 340°C	1.36×10^{-5}	1.33
B40	τ_{imp} = 3s, T_S = 340°C	5.94×10^{-5}	1.27
	τ_{imp} = 7s, T_S = 340°C	1.40×10^{-5}	1.35
B50	τ_{imp} = 3s, T_S = 340°C	2.83×10^{-6}	1.60
	τ_{imp} = 7s, T_S = 340°C	3.86×10^{-6}	1.49

4. Conclusions

Neat diesel fuel and Malaysian palm oil biodiesel-diesel blend fuel (B10-B50) had their droplet evaporation characteristics on a heated aluminum alloy plate analyzed and compared to each other. The following is a summary of the main findings:

i. HSDT is a suitable method to evaluate the single droplet evaporation characteristics of fuel.
ii. For some fuels, the properties in terms of blending ratio did not have a significant impact on the droplet MEP. The MEP obtained for the tested fuels were 360°C (DF), 365°C (B10 and B50), 375°C (B20 and B40), and 385°C (B30).
iii. DF droplet evaporation produced the most droplet splashes and smoke during the evaporation test. Splashes could cause the fuel remains to stick on the surface wall and might increase deposit formation.

iv. The fuel evaporation characteristics provided information about the initial wetting condition, droplet physical interaction with the hot surface, and droplet lifetime estimation that can be used to explain deposit formation on the hot surface.
v. The evaporation profiles indicated that as the temperature of the hot plate increases, the evaporation lifetime of the fuel droplet for each test fuel decreases. This shows the effect of temperature which caused fuel to evaporate faster at higher temperatures.
vi. Thicker deposits exhibit lower surface temperatures due to their poor thermal conductivity. This, in turn, makes it more challenging for subsequent fuel droplets that come into contact with them to vaporize, ultimately leading to an increased generation of deposits.
vii. There was a significant impact of the biodiesel content in the B10-B50 especially on the deposition rate. It has been found that fuel with higher biodiesel content tends to generate more deposits at a faster deposition rate.

Acknowledgement

This work was supported by Fundamental Research Grant Scheme (FRGS) – FRGS/1/2020/TK0/UTEM/02/20. The authors would like to thank the staff of the Faculty of Mechanical Technology and Engineering, Universiti Teknikal Malaysia Melaka for their support.

References

[1] Vergel-Ortega, Mawency, Guillermo Valencia-Ochoa, and Jorge Duarte-Forero. "Experimental study of emissions in single-cylinder diesel engine operating with diesel-biodiesel blends of palm oil-sunflower oil and ethanol." *Case Studies in Thermal Engineering* 26 (2021): 101190. https://doi.org/10.1016/j.csite.2021.101190
[2] Pourhoseini, S. H., and Maryam Ghodrat. "Experimental investigation of the effect of Al2O3 nanoparticles as additives to B20 blended biodiesel fuel: Flame characteristics, thermal performance and pollutant emissions." *Case Studies in Thermal Engineering* 27 (2021): 101292. https://doi.org/10.1016/j.csite.2021.101292
[3] Rahman, Nik Kechik Mujahidah Nik Abdul, Syamimi Saadon, and Mohd Hasrizam Che Man. "Waste Heat Recovery of Biomass Based Industrial Boilers by Using Stirling Engine." *Journal of Advanced Research in Fluid Mechanics and Thermal Sciences* 89, no. 1 (2022): 1-12. https://doi.org/10.37934/arfmts.89.1.112
[4] Jikol, F., M. Z. Akop, Y. M. Arifin, M. A. Salim, and S. G. Herawan. "Biofuel Development in Malaysia: Challenges and Future Prospects of Palm Oil Biofuel." *International Journal of Nanoelectronics & Materials* 15 (2022).
[5] Maksom, Mohammad Syahadan, Nurul Fitriah Nasir, Norzelawati Asmuin, Muhammad Faqhrurrazi Abd Rahman, and Riyadhthusollehan Khairulfuaad. "Biodiesel composition effects on density and viscosity of diesel-biodiesel blend: a CFD study." *CFD Letters* 12, no. 4 (2020): 100-109. https://doi.org/10.37934/cfdl.12.4.100109
[6] Sarwani, Muhamad Khairul Ilman, Mas Fawzi, Shahrul Azmir Osman, Anwar Syahmi, and Wira Jazair Yahya. "Calculation of Specific Exhaust Emissions of Compression Ignition Engine Fueled by Palm Biodiesel Blend." *Journal of Advanced Research in Applied Sciences and Engineering Technology* 27, no. 1 (2022): 92-96. https://doi.org/10.37934/araset.27.1.9296
[7] Zulkurnai, Fatin Farhanah, Norhidayah Mat Taib, Wan Mohd Faizal Wan Mahmood, and Mohd Radzi Abu Mansor. "Combustion characteristics of diesel and ethanol fuel in reactivity controlled compression ignition engine." *Journal of Advanced Research in Numerical Heat Transfer* 2, no. 1 (2020): 1-13.
[8] Marlina, Ena, W. Wijayanti, L. Yuliati, and I. N. G. Wardana. "The role of pole and molecular geometry of fatty acids in vegetable oils droplet on ignition and boiling characteristics." *Renewable Energy* 145 (2020): 596-603. https://doi.org/10.1016/j.renene.2019.06.064
[9] Marlina, Ena, W. Wijayanti, Lilis Yuliati, and I. N. G. Wardana. "The role of 1.8-cineole addition on the change in triglyceride geometry and combustion characteristics of vegetable oils droplets." *Fuel* 314 (2022): 122721. https://doi.org/10.1016/j.fuel.2021.122721
[10] Jikol, F., M. Z. Akop, Y. M. Arifin, M. A. Salim, and S. G. Herawan. "Deposits Formation, Emissions, and Mechanical Performance of Diesel Engine Fuelled with Biodiesel: A Review." *International Journal of Nanoelectronics & Materials* 15 (2022).
[11] Faik, Ahmad Muneer El-Deen, Yang Zhang, and Sérgio de Morais Hanriot. "Droplet Combustion Characteristics of Biodiesel-Diesel Blends using High Speed Backlit and Schlieren Imaging." *Heat Transfer Engineering* 40, no. 13-14 (2019): 1085-1098. https://doi.org/10.1080/01457632.2018.1457209
[12] Pan, Yaoyu, Xiufeng Yang, Song-Charng Kong, Foo Chern Ting, Claudia Iyer, and Jianwen Yi. "Characterization of fuel

drop impact on wall films using SPH simulation." *International Journal of Engine Research* 23, no. 3 (2022): 416-433. https://doi.org/10.1177/1468087421992888

[13] Won, Jonghan, Seung Wook Baek, Hyemin Kim, and Hookyung Lee. "The viscosity and combustion characteristics of single-droplet water-diesel emulsion." *Energies* 12, no. 10 (2019): 1963. https://doi.org/10.3390/en12101963

[14] Mariani, Valerio, Gian Marco Bianchi, Giulio Cazzoli, and Stefania Falfari. "Fuel droplet-wall impingement under GDI-like conditions: A numerical investigation." In *AIP Conference Proceedings*, vol. 2191, no. 1. AIP Publishing, 2019. https://doi.org/10.1063/1.5138840

[15] Aggarwal, Suresh K. "Single droplet ignition: Theoretical analyses and experimental findings." *Progress in Energy and Combustion Science* 45 (2014): 79-107. https://doi.org/10.1016/j.pecs.2014.05.002

[16] Wang, Jigang, Xiaoyu Huang, Xinqi Qiao, Dehao Ju, and Chunhua Sun. "Experimental study on evaporation characteristics of single and multiple fuel droplets." *Journal of the Energy Institute* 93, no. 4 (2020): 1473-1480. https://doi.org/10.1016/j.joei.2020.01.009

[17] Zhang, Yu, Ronghua Huang, Yuhan Huang, Sheng Huang, Pei Zhou, Xi Chen, and Tian Qin. "Experimental study on combustion characteristics of an n-butanol-biodiesel droplet." *Energy* 160 (2018): 490-499. https://doi.org/10.1016/j.energy.2018.07.039

[18] Wang, Fang, Rui Liu, Min Li, Jie Yao, and Jie Jin. "Kerosene evaporation rate in high temperature air stationary and convective environment." *Fuel* 211 (2018): 582-590. https://doi.org/10.1016/j.fuel.2017.08.062

[19] He, Ming, and Ying Piao. "An Experimental Study on the Phenomena inside the Burning Aviation Kerosene Droplet." *Journal of Thermal Science* 30 (2021): 2202-2213. https://doi.org/10.1007/s11630-021-1408-5

[20] Segawa, Daisuke, Toshikazu Kadota, Shinji Nakaya, Kazuma Takemura, and Taketsugu Sasaki. "A liquid film or droplet of miscible binary fuel burning on a heated surface at elevated pressures." *Proceedings of the Combustion Institute* 32, no. 2 (2009): 2187-2194. https://doi.org/10.1016/j.proci.2008.06.080

[21] Orzechowski, Tadeusz. "Leidenfrost evaporation of a single droplet of gasoline blends of ethanol." In *EPJ Web of Conferences*, vol. 213, p. 02062. EDP Sciences, 2019. https://doi.org/10.1051/epjconf/201921302062

[22] Mohaddes, Danyal, Philipp Boettcher, and Matthias Ihme. "Hot surface ignition of a wall-impinging fuel spray: Modeling and analysis using large-eddy simulation." *Combustion and Flame* 228 (2021): 443-456. https://doi.org/10.1016/j.combustflame.2021.02.025

[23] Mach, Thomas J., Rodney L. Sung, Peter M. Liiva, William P. Acker, J. Christian Swindal, and Richard K. Chang. *Experimental determination of fuel additive effects on Leidenfrost temperature and deposit formation*. No. 930774. SAE Technical Paper, 1993. https://doi.org/10.4271/930774

[24] Reis, Max William Frasão. "Study of the Boiling Phenomenon Using the Droplet Evaporation Method." *Campinas State University* (2019): 1-93.

[25] Bertola, V. "An impact regime map for water drops impacting on heated surfaces." *International Journal of Heat and Mass Transfer* 85 (2015): 430-437. https://doi.org/10.1016/j.ijheatmasstransfer.2015.01.084

[26] Chausalkar, Abhijeet, Chol-Bum M. Kweon, Song-Charng Kong, and James B. Michael. "Leidenfrost behavior in drop-wall impacts at combustor-relevant ambient pressures." *International Journal of Heat and Mass Transfer* 153 (2020): 119571. https://doi.org/10.1016/j.ijheatmasstransfer.2020.119571

[27] Liang, Gangtao, and Issam Mudawar. "Review of drop impact on heated walls." *International Journal of Heat and Mass Transfer* 106 (2017): 103-126. https://doi.org/10.1016/j.ijheatmasstransfer.2016.10.031

[28] Ali, Obed M., Rizalman Mamat, Nik R. Abdullah, and Abdul Adam Abdullah. "Analysis of blended fuel properties and engine performance with palm biodiesel-diesel blended fuel." *Renewable Energy* 86 (2016): 59-67. https://doi.org/10.1016/j.renene.2015.07.103

[29] Arifin, Yusmady Mohamed, and Masataka Arai. "Deposition characteristics of diesel and bio-diesel fuels." *Fuel* 88, no. 11 (2009): 2163-2170. https://doi.org/10.1016/j.fuel.2009.01.021

[30] Pham, Van Viet. "Analyzing the effect of heated wall surface temperatures combustion chamber deposit formation." *Journal of Mechanical Engineering Research & Developments (JMERD)* 41, no. 4 (2018): 17-21. https://doi.org/10.26480/jmerd.04.2018.17.21

[31] Suryantoro, M. T., H. Setiapraja, S. Yubaidah, Bambang Sugiarto, A. B. Mulyono, M. I. Attharik, T. Halomoan, and M. R. Ariestiawan. "Effect of temperature to diesel (B0) and biodiesel (B100) fuel deposits forming." In *AIP Conference Proceedings*, vol. 2062, no. 1. AIP Publishing, 2019. https://doi.org/10.1063/1.5086591

[32] Pham, Van Viet. "Research and design an experimental model for the determination of deposits formation mechanism in the combustion chamber." *International Journal on Advanced Science Engineering and Information Technology* 9, no. 2 (2019): 656-663. https://doi.org/10.18517/ijaseit.9.2.8361

[33] Doetein, Isaac, Lutendo Muremi, and Pitshou Bokoro. "An Analysis of geometry characteristics of metal oxide blocks on heat flow rate using Finite Element Analysis." In *2020 IEEE Electrical Insulation Conference (EIC)*, pp. 163-166. IEEE, 2020. https://doi.org/10.1109/EIC47619.2020.9158759

[34] Srikanth, P. V., B. V. V. P. Rao, K. M. Laxmi, and N. HariBabu. "Material coating optimization and thermal analysis of

a four stroke CI engine piston." *International Journal of Mechanical Engineering and Technology* 8, no. 8 (2017): 988-997.

[35] Jikol, F., M. Z. Akop, Y. M. Arifin, M. A. Salim, and S. G. Herawan. "A Study of Steady-State Thermal Distribution on Circular Plate Using ANSYS." *International Journal of Nanoelectrics and Materials* 14 (2021): 479-488.

[36] Jikol, F., M. Z. Akop, Y. M. Arifin, M. A. Salim, and S. G. Herawan. "Transient Thermal Analysis on Convection Process of Circular Plate Used in Hot Surface Deposition Test Rig." *International Journal of Nanoelectronics & Materials* 15 (2022).

[37] Fukuda, Shinya, Masamichi Kohno, Keisuke Tagashira, Nobuya Ishihara, Sumitomo Hidaka, and Yasuyuki Takata. "Behavior of small droplet impinging on a hot surface." *Heat Transfer Engineering* 35, no. 2 (2014): 204-211. https://doi.org/10.1080/01457632.2013.812496

[38] Arifin, Yusmady Mohamed, and Masataka Arai. "The effect of hot surface temperature on diesel fuel deposit formation." *Fuel* 89, no. 5 (2010): 934-942. https://doi.org/10.1016/j.fuel.2009.07.014

[39] Khavari, Mohammad, Chao Sun, Detlef Lohse, and Tuan Tran. "Fingering patterns during droplet impact on heated surfaces." *Soft Matter* 11, no. 17 (2015): 3298-3303. https://doi.org/10.1039/C4SM02878C

[40] Bernardin, John D., Clinton J. Stebbins, and Issam Mudawar. "Mapping of impact and heat transfer regimes of water drops impinging on a polished surface." *International Journal of Heat and Mass Transfer* 40, no. 2 (1997): 247-267. https://doi.org/10.1016/0017-9310(96)00119-6

[41] Senda, Jiro, Tomoyuki Kanda, Marwan Al-Roub, Patrick V. Farrell, Takashi Fukami, and Hajime Fujimoto. *Modeling Spray Impingement Considering Fuel Film Formation on the Wall*. No. 970047. SAE Technical Paper, 1997. https://doi.org/10.4271/970047

[42] Senda, Jiro, Koji Yamada, Hajime Fujimoto, and Hideo Miki. "The heat-transfer characteristics of a small droplet impinging upon a hot surface." *JSME International Journal. Ser. 2, Fluids Engineering, Heat Transfer, Power, Combustion, Thermophysical Properties* 31, no. 1 (1988): 105-111. https://doi.org/10.1299/jsmeb1988.31.1_105

[43] Arifin, Yusmady Mohamed, Tomohiko Furuhata, Masahiro Saito, and Masataka Arai. "Diesel and bio-diesel fuel deposits on a hot surface." *Fuel* 87, no. 8-9 (2008): 1601-1609. https://doi.org/10.1016/j.fuel.2007.07.030

[44] Zare, Mehdi, Barat Ghobadian, Seyed Reza Hassan-Beygi, and Gholamhasan Najafi. "Evaporation Characteristics of Diesel and Biodiesel Fuel Droplets on Hot Surfaces." *Journal of Renewable Energy and Environment* 7, no. 2 (2020): 1-7.

[45] Kompinsky, E., G. Dolan, and E. Sher. "Experimental study on the dynamics of binary fuel droplet impacts on a heated surface." *Chemical Engineering Science* 98 (2013): 186-194. https://doi.org/10.1016/j.ces.2013.04.047

[46] Wang, Zhenying, Daniel Orejon, Yasuyuki Takata, and Khellil Sefiane. "Wetting and evaporation of multicomponent droplets." *Physics Reports* 960 (2022): 1-37. https://doi.org/10.1016/j.physrep.2022.02.005

[47] Furuhata, Tomohiko, Takeshi Ohmori, and Masataka Arai. *Evaporation deposits of diesel and bio-diesel fuels on a hot surface*. No. 2011-01-1933. SAE Technical Paper, 2011. https://doi.org/10.4271/2011-01-1933

[48] Mohamed Arifin, Y., Y. Tsuruta, T. Furuhata, M. Saito, and M. Arai. "Influence factors of deposits formation on a hot surface for diesel and bio-blended diesel fuel." In *The Seventh International Conference on Modeling and Diagnostics for Advanced Engine Systems (COMODIA 2008)*, pp. 799-805. 2008. https://doi.org/10.1299/jmsesdm.2008.7.799